Journal Pre-proofs

Research Article

Dynamic changes in synaptic plasticity genes in ipsilateral and contralateral inferior colliculus following unilateral noise-induced hearing loss

Senthilvelan Manohar, Francesca Yoshie Russo, Gail M. Seigel, Richard Salvi

Please cite this article as: S. Manohar, F. Yoshie Russo, G.M. Seigel, R. Salvi, Dynamic changes in synaptic plasticity genes in ipsilateral and contralateral inferior colliculus following unilateral noise-induced hearing loss, *Neuroscience* (2020), doi: https://doi.org/10.1016/j.neuroscience.2020.04.010

This is a PDF file of an article that has undergone enhancements after acceptance, such as the addition of a cover page and metadata, and formatting for readability, but it is not yet the definitive version of record. This version will undergo additional copyediting, typesetting and review before it is published in its final form, but we are providing this version to give early visibility of the article. Please note that, during the production process, errors may be discovered which could affect the content, and all legal disclaimers that apply to the journal pertain.
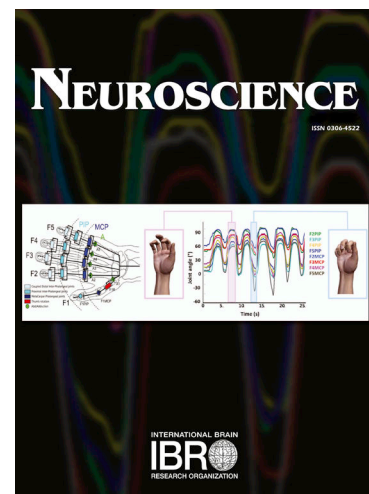
Dynamic changes in synaptic plasticity genes in ipsilateral and contralateral inferior colliculus following unilateral noise-induced hearing loss

Senthilvelan Manohar, Francesca Yoshie Russo[#], Gail M. Seigel and Richard Salvi [*]

[#]current address: Department of Sense Organs, Sapienza University of Rome, Rome, Italy

[*]Corresponding author: Richard Salvi, University at Buffalo, Center for Hearing and Deafness, 137 Cary Hall, Buffalo, NY 14214; email: salvi@buffalo.edu

List of uncommon abbreviations

ABR   Auditory brain stem response

ANOVA   Analysis of variance

Ct   Cycle threshold

dB   Decibels

DCN   Dorsal cochlear nucleus

FC   Fold change

GABA   Gamma-Aminobutyric Acid

Hz   Hertz

IEG   Immediate early gene

LRG   Late response gene

LTD   Long term depression

LTP   Long term potentiation

SEM   Standard error of the mean

SPL   Sound pressure level

VCN   Ventral cochlear nucleus

Abstract

Unilateral noise-induced hearing loss reduces the input to the central auditory pathway disrupting the excitatory and inhibitory inputs to the inferior colliculus (IC), an important binaural processing center. Little is known about the compensatory synaptic changes that occur in the IC as a consequence of unilateral noise-induced hearing loss. To address this issue, Sprague-Dawley rats underwent unilateral noise exposure resulting in severe unilateral hearing loss. IC tissues from the contralateral and ipsilateral IC were evaluated for acute (2-d) and chronic (28-d) changes in the expression of 84 synaptic plasticity genes on a PCR array. *Arc* and *Egr1* gene were further visualized by *in situ* hybridization to validate the PCR results. None of the genes were upregulated, but many were downregulated post-exposure. At 2-d post-exposure, more than 75% of the genes were significantly downregulated in the contralateral IC, while only two were downregulated in the ipsilateral IC. Many of the downregulated genes were related to long-term depression, long-term potentiation, cell adhesion, immediate early genes, neural receptors and postsynaptic density. At 28-d post-exposure, the gene expression pattern was reversed with more than 85% of genes in the ipsilateral IC now downregulated. Most genes previously downregulated in the contralateral IC 2-d post-exposure had recovered; less than 15% remained downregulated. These time-dependent, asymmetric changes in synaptic plasticity gene expression could shed new light on the perceptual deficits associated with unilateral hearing loss and the dynamic structural and functional changes that occur in the IC days and months following unilateral noise-induced hearing loss.

Keywords: Inferior colliculus; noise exposure; unilateral hearing loss; synaptic plasticity; gene expression, mRNA

Introduction

Two ears are better than one in nearly all aspects of auditory perception, but especially when it comes to sound localization. The auditory system is able to precisely identify the location of a sound source in space using extremely small interaural time differences (ITD) and interaural intensity differences (IID) (Blauert, 1983). The initial stages of binaural processing needed to localize a sound are accomplished by neurons located in the superior olivary complex and inferior colliculus (IC). Binaurally sensitive neurons in these regions are extraordinarily sensitive to small ITDs and IITs (Yin and Chan, 1990, Li and Kelly, 1992, Park and Pollak, 1993). Consequently, severe unilateral hearing loss would be expected to disrupt the magnitude and time of arrival of the synaptic inputs that impinge upon binaural neurons in the auditory brainstem and midbrain. The loss of auditory information from one ear would also likely disrupt the integration of sound-evoked neural activity with visual and somatosensory system (Aitkin et al., 1978, Brainard and Knudsen, 1995).

The IC plays an important role in many aspects of auditory processing such as intensity coding, temporal processing, sound localization and multisensory integration (Popelar et al., 1994, Spongr et al., 1997, Walton et al., 1998, Horvath and Lesica, 2011, Nakamoto et al., 2015). Unilateral noise-induced hearing loss (NIHL) leads to transneuronal axonal degeneration in both the ipsilateral and contralateral IC (Kim et al., 1997, Morest et al., 1997) and a gradual increase in sound-evoked hyperactivity in the ipsilateral IC and an increase in spontaneous activity in both the ipsilateral and contralateral IC over several weeks (Popelar et al., 1994, Mulders and Robertson, 2009). Unilateral cochlear damage results in a significant decrease immunolabeling of GABA receptors in the contralateral IC (Dong et al., 2010b).

The functional and structural changes resulting from cochlea damage likely leads to altered gene expression in the IC. In one study, high-frequency, unilateral noise-induced hearing loss altered the expression level of eight candidate genes in the IC. Immediately after the noise-exposure when thresholds were elevated approximately 65 dB, the mRNA levels of

4

genes involved in excitatory and inhibitory neurotransmission were downregulated in both the ipsilateral and contralateral IC (Dong et al., 2010a). After a 4-week recovery period, hearing thresholds and gene expression levels had largely recovered to their original levels. These results suggest that the noise-induced gene expression changes related to neurotransmission vary with post-exposure time in both the ipsilateral and contralateral IC. Therefore, we designed our study to examine both early and late changes in synaptic plasticity gene expression in both the ipsilateral and contralateral IC following a severe unilateral noise exposure.

Except for a few studies that assessed a handful of genes (Dong et al., 2010a, Dong et al., 2010b, Vogler et al., 2014), almost nothing is known about the dynamic changes in gene expression that occur in the IC following permanent unilateral NIHL. The dynamic changes in gene expression that occur after a severe unilateral hearing loss almost certainly contribute to the structural and functional remodeling of the synapses in the ipsilateral and contralateral IC that are involved with complex perceptual processes such as sound localization, intensity coding, multisensory integration and tinnitus. Determining which synaptic plasticity genes are involved in remodeling the neural circuits in the ipsilateral and contralateral IC could provide novel insights into the mechanisms that drive the neuroplastic changes in the IC following unilateral hearing loss.

To address this knowledge gap, we focused our efforts on identifying changes in 84 synaptic plasticity genes that likely contribute to the functional and structural reorganization of the IC following severe unilateral hearing loss. Intense noise exposure was used to induce unilateral hearing loss because it is one of the most common causes of acquired hearing loss in young adults and military personnel (Humes et al., 2006, Moon, 2007). In addition, unilateral noise-induced hearing loss is often used to induce tinnitus (Heffner and Harrington, 2002) and to investigate its neural correlates during the acute and chronic stages of the disorder (Ma et al., 2006, Mulders and Robertson, 2009). Therefore, we unilaterally exposed rats to intense noise (126 dB SPL) that induced a severe unilateral hearing loss. Afterwards we evaluated the acute

(2-d) and chronic (28-d) changes in the expression of 84 synaptic plasticity-related genes in both the contralateral and ipsilateral IC.

Methods

Subjects: All procedures used in this study were approved by the University at Buffalo Institutional Animal Care and Use Committee and were consistent with NIH guidelines. Sprague-Dawley rats, 3-4 months of age, were used for these studies. The rats were housed in the University at Buffalo Laboratory Animals Facility and given free access to food and water. The colony was maintained at 22°C and followed a 12-h light/dark cycle. A total of 15 rats were used. Six rats were used for auditory brainstem response (ABR) hearing tests and *in situ* hybridization studies (three controls and three 28-d post-exposure). The ABR was used to estimate the hearing loss in the noise-exposed ear and the contralateral ear that was ear-pugged during the noise exposure as described below. To avoid the confounding effects of anesthesia and the stress associated with ABR testing, the remaining nine rats were used exclusively for the gene array studies (three controls, three 2-d post-exposure and three 28-d post-exposure.

Noise exposure: The noise-exposed rats and sham control rats were anesthetized with isoflurane (1.5%). The left ear of the noise-exposed rats were exposed for 2 h to at 126 dB SPL narrow band noise (NBN, 100 Hz bandwidth) centered at 12 kHz as described previously (Kraus et al., 2011, Baizer et al., 2015). The output port of the super compression acoustic driver was placed approximately 10 mm from the opening of the left ear canal. The left ear was chosen for the exposure because of logistical consideration related to the equipment and to optimize reliability and consistency in the results. A foam plug was securely inserted into the contralateral ear canal and then completely covered with petroleum jelly to protect the right ear from noise damage (Kraus et al., 2011, Manohar et al., 2016). Because the exposure intensity was extremely high and the sound source was oriented close to the entrance of the ear canal, noise-exposed ears were expected to sustain massive hair cell lesion and significant hearing

6

loss at all frequencies whereas hair cells and auditory thresholds were expected to remain normal in the plugged ears as previously reported (Kraus et al., 2011, Baizer et al., 2015, Manohar et al., 2016). Sham control rats underwent the same procedure, but without the noise exposure. The noise exposure and sham experimental treatments were carried out at approximately the same time of day (between 10:00 am and 12:30 pm).

Auditory Brainstem Response (ABR): The auditory brainstem response (ABR) was measured in three unilaterally noise-exposed rats and three sham controls using methods described previously (Jamesdaniel et al., 2008, Chen et al., 2010, Liu et al., 2011). The experimenter measuring the ABR thresholds was blind to the experimental treatment. Briefly, the rats were anesthetized with ketamine (50 mg/kg, i.p.) and xylazine (6 mg/kg) (i.p.) and placed on a heating pad to maintain core body temperature at 37 °C. ABR threshold measurements were obtained from both the left and right ear. During ABR testing, a foam earplug was inserted securely into the contralateral, non-test ear and covered with petroleum jelly while tone-bursts were presented to the ipsilateral test ear. After completing the ABR testing in ipsilateral test ear, the earplug material was removed and placed in the opposite ear and tone bursts presented to the unplugged test ear to determine the ABR thresholds in that ear. Digitally generated (TDT system, SigGen, FL, USA) tone bursts (1 ms duration, 0.5 ms rise/fall time, $cosine^2$-gated, 6, 12, 20, and 32 kHz) were presented at a rate of 21/s through a loudspeaker (FT28D, Fostex) located approximately 15 cm from the opening of the ear canal of the test ear. The sound level was decreased in 10 dB increments from 90 dB SPL to at least 10 dB below the intensity at which the ABR response disappeared. Threshold was defined as the lowest intensity needed to reliably obtain a just detectable ABR response consisting of a positive to negative deflection in ABR waveform that typically occurred around 4-5 ms after stimulus onset (Jamesdaniel et al., 2008, Chen et al., 2014). ABR thresholds were measured in the left and right ears at 28-d post-treatment in both noise-exposed group and sham groups.

7

Synaptic Plasticity qRT-PCR: Nine rats (three sham controls, three noise-exposed rats at 2-d post-treatment and three noise-exposed rats at 28 d post-treatment) were used for the gene array studies. The researcher carrying out the gene array studies was blind to the experimental treatment. Our qRT-PCR procedures are described in detail in previous publications (Hu et al., 2009, Manohar et al., 2014, Manohar et al., 2016, Manohar et al., 2019). To harvest the tissues as quickly as possible, the rats were euthanized with CO_2, decapitated and the brain rapidly removed. The left and right ICs were carefully dissected out in an RNase free environment. Total RNA was isolated from the tissues using the RNeasy extraction kit (Qiagen) as described previously (Manohar et al., 2016, Manohar et al., 2019)

The noise-induced gene expression changes in the IC were evaluated using a synaptic plasticity gene array (RT^2 Profiler PCR Array Rat Synaptic Plasticity, Cat. no: PARN-126ZA array, SA Biosciences/Qiagen) according to the manufacturer's instructions. A list of gene abbreviations with outlinks to definitions and annotations are available at: https://tinyurl.com/y9py9843. PCR analysis was performed with a Bio-Rad CFX Connect Real Time PCR System (Manohar et al., 2016, Manohar et al., 2019). Three samples each from different animals were evaluated for the experimental conditions (sham control, 2-d post-exposure, and 28-d post-exposure). Fold changes and the statistical analysis of noise-induced changes in mRNA expression levels in the IC were performed using the SA Biosciences online data analysis resource (https://geneglobe.qiagen.com/us/analyze/). Details of the company's optimized data analysis procedures can be found on the company's web site. The software evaluates the efficiency and stability of the five housekeeping genes across the samples and uses this information to compute gene expression levels and optimize the data analysis. Noise-induced changes in gene expression were considered significant if: (1) the FC in gene expression increased by more than 50% or decreased by more than 50% (i.e., -0.5 < FC >0.5) and (2) $p<0.05$ for statistical comparison. Differential expression of mRNAs associated with synaptic plasticity was expressed in a volcano plot. Fold changes (FC) and p values were

8

converted into log 2 and – log 10 values in volcano plot, respectively. In addition, a qRT-PCR synaptic plasticity gene profile analysis was performed on the sham controls to characterize the relative abundance of the synaptic plasticity genes relative to the housekeeping gene actin in the IC. Actin was used quantify the relative abundance of the synaptic plasticity genes because: (1) actin is one of the most highly abundant and stable housekeeping genes and (2) actin was used in our previous gene profiling studies of the dorsal and ventral cochlear nucleus to quantify the relative abundance of synaptic plasticity genes and genes involved in inflammation, pain and GABAergic neurotransmission (Manohar et al., 2016, Manohar et al., 2019).

RNA *In Situ* Hybridization: Six rats (tissues were harvested from three sham control rats, and three noise-exposed rats at 28-d post-exposure) were used for the RNA *in situ* hybridization studies following procedures described in our previous study (Manohar et al., 2019). The rats were euthanized with 86 mg/kg, i.p, Fatal Plus (Vortech Pharmaceutical Ltd.) and perfused with 0.1 M phosphate buffered saline (PBS) followed by 10% formalin in PBS. The brains were removed, post-fixed with 10% formalin for 24 h, and then cryoprotected in 15% sucrose in PBS for 6 h followed by 30% sucrose in PBS for 12 h. Frozen sections were cut at a thickness of 15 μm, mounted on Superfrost Plus slides (Thermo Fischer Scientific) and stored at -80 $^{\circ}$C for later processing. Slides were processed according to the kit instructions (Advanced Cell Diagnostics, Newark, CA, RNAscope). The technician processing the brain sections for in situ hybridization was blind to the experimental treatment. Probes for *Arc, and Egr1* as well as the ubiquitin (*Ubc*) control probes were evaluated using 15 μm thick cryostat sections from the inferior colliculus. Labeled sections were counterstained with Gills' hematoxylin (RICC Chemical Co., Arlington, TX). Sections were visualized with a light microscope (Zeiss Axioskop, 400X) and photographed with a digital camera (SPOT Insight, Diagnostic Instruments Inc.).

9

Statistics and Gene Array Analysis: For gene array analysis, p-values were calculated using SA Biosciences online software (https://geneglobe.qiagen.com/us/analyze/) that uses a Student's t-test (two-tail distribution, equal variances between two samples, without correction for multiple comparisons) on the replicate $2^{-\Delta CT}$ values for each gene. To reduce the likelihood of false positives, we used two criteria to classify noise-induced changes in gene expression as significant: (1) the FC in gene expression had to have increased by more than 50% or decreased by more than 50% (i.e., -0.5 < FC >0.5) and (2) the t-tests from the online analysis had to return a p value of p <0.05 as described in our previous publication (Manohar et al., 2019).

Results

Noise-Induced Unilateral Hearing Loss: The 126 dB SPL unilateral noise exposure (2 h, 12 kHz NBN) caused profound unilateral hearing loss. Figure 1A compares the mean (+/- SD, n=3) ABR thresholds evoked by sound stimulation delivered to the left ear of the rats that were noise-exposed in the left ear versus those evoked by sounds presented to the left ear of the sham control rats. ABR thresholds in the left ear of the noise exposed rats ranged from ~90-100 dB SPL at frequencies from 6 to 32 kHz. ABR thresholds in the left ear of the noise-exposed rats were 50-60 dB higher than those in the left ear of the sham control rats confirming that the noise exposure had induced a severe unilateral hearing loss. To determine if the unilateral exposure to the left ear affected thresholds in the plugged right ear, we compared the ABR thresholds in the right, plugged ear of the noise-exposed rats with right ear of the sham control rats; ABR thresholds for the two groups were nearly identical (Figure 1B). The ABR data confirmed that the 126 dB SPL exposure induced a significant hearing loss in the left-exposed ear, but did not affect ABR thresholds in the right ear that was plugged during the noise exposure. The large ABR thresholds shift in the left, noise-exposed ears are consistent with the massive hair cell lesions and nerve fiber lesions induced by this exposure (Kraus et al., 2011, Baizer et al., 2015).

IC Synaptic Plasticity Gene Profile: The synaptic plasticity gene profile can be used to assess the relative abundance of each of the 84 mRNA being produced by the cells within the IC of control animals under normal conditions. The information in mRNA for making a specific synaptic protein is transferred into the cytoplasm where it interacts with a ribosome that translates the sequence of mRNA bases into sequence of three base codons that are compiled into a series of amino acids needed to assemble a specific protein. In most cells, translation largely occur on ER-bound ribosome and freely diffusing cytosolic ribosomes; however, in neurons, mRNA packaged in granules are translated in proximal dendrites and also distant dendrites where they can be synthesized in the appropriate location as needed (Wu et al., 2016).

The relative abundance of these genes under normal conditions, putatively indicative of normal protein requirements of the cell, could be helpful for interpreting the gene expression changes that occur after an experimental manipulation. Therefore, we calculated the relative abundance of the 84 synaptic plasticity genes in the IC of the three sham control rats by normalizing the value of each synaptic plasticity gene to the value of the highly abundant actin housekeeping gene. Table 1 shows the relative abundance of each of the 84 synaptic plasticity genes compared to the highly abundant actin housekeeping gene. The 10 most abundant genes are highlighted in bold. Among the top five synaptic plasticity genes in Table 1, the most abundant was *Rab3a;* its relative abundance compared to actin was 0.418 (i.e., 41.8% relative to actin). The second most abundant gene was *Gria2* (0.201 or 20.1%), which encodes the excitatory glutamate ionotropic AMPA receptor subunit 2 (Chen et al., 2001). Ppp3ca (Protein Phosphatase 3 Catalytic Subunit Alpha), the third most abundant gene (0.149 or 14.9%) codes for subunits of calcineurin A, a protein involved in the transduction of intracellular calcium-mediated signals (Wang et al., 1996). The fourth most abundant gene, *Mapk1* (0.134 or 13.4%), codes for mitogen-activate protein kinase 1 (also known as ERK2), which is involved in proliferation, differentiation and transcription. The fifth most abundant gene was *Ywhaq* (0.126

11

or 12.6%), which codes a family of 14-3-3 proteins involved in signal transduction, apoptosis

and proliferation (Malaspina et al., 2000).

Gene Expression Changes in Ipsilateral IC 2-d Post-Exposure: To help with

interpretation of the noise-induced gene expression data, the 84 synaptic plasticity genes were

organized by the gene array manufacturer into nine defined functional categories and an "other"

category. The functional categories in Table 2 are: long term depression (LTD), long term

potentiation (LTP), immediate early gene (IEG), late response gene (LRG), cell adhesion (CA),

extracellular matrix and proteolytic activity (EMP), Creb cofactors (CC), neuronal receptors

(NR), postsynaptic density (PSD) and other (OT). Not surprisingly, many genes are involved in

several different functions and therefore some genes are represented in multiple categories in

Table 2. We retained these nine categories so that the results from the IC can be compared to

our previous noise-induced results from the cochlear nucleus (Manohar et al., 2019).

The 2-d post-exposure gene expression data for the ipsilateral IC are presented in the

volcano plot of Figure 2A. The p-values on the ordinate are expressed in $-\text{Log}_{10}$ format. The

abscissa shows the fold change in gene expression in Log_2 format. Points to the right of the

right, vertical red line represent gene expression increases greater than 50% (FC=1.5; $\log_2(1.5)$

= 0.5849). Points to the left of the left, dashed blue line represent gene expression decreases

greater than 50% (FC=0.5; $\log_2(0.5)$ = -1). Those points that met the >50% or <50% criterion

and that were above the horizontal, green dashed line identify statistically significant changes in

gene expression (p<0.05). In the ipsilateral IC, no genes were significantly upregulated at 2-

days post-exposure; however, two genes, *Tnf*, and *Ngfr,* were significantly downregulated at this

time (Table 3)*. Tnf* encodes a multifunctional proinflammatory cytokine that belongs to the

tumor necrosis factor (TNF) superfamily; this TNF cytokine is mainly secreted by macrophages

(Cox et al., 1990) and brain microglia (Olmos and Llado, 2014), as well as other immune cells

(Broudy et al., 1987) and neurons (Lim et al., 2016). The *Ngfr* gene codes for the nerve growth

factor receptor (NGFr). Nerve growth factor (NGF) binds to NGFr with high affinity (Wyatt et al.,

1990) and promotes neuronal survival and differentiation. The *tnf* gene was listed in the cell adhesion category and *ngfr* was listed in the LTD category (Table 2) per the manufacturer's data sheet, but could also be place in other categories.

Gene Expression Changes in Contralateral IC 2-d Post-Exposure: The 2-d post-exposure gene expression data for the contralateral IC are presented in the volcano plot of Figure 2B. None of the genes were upregulated in the contralateral IC. However, 65 of 84 genes were significantly downregulated (Table 4). The decreases in gene expression were quite large; 10 genes (*Arc, Grin2d, Grm2, Grm5, Junb, Nfkb1, Ngfr, Pcdh8, Plcg1 and Tnf*) were downregulated more than 5 fold (FC<0.2; $\log_2 (0.2) = -2.3219$). The numbers of downregulated genes in the 10 categories (Table 2) were: 22 were in the LTD category, 19 in LTP, 21 in IER, 1 in LRG, 9 in CA, 2 in EMP, 6 in CC, 18 in NR, 13 in PSD and 2 in OT.

Gene Expression Changes in Ipsilateral IC 28-d Post-Exposure: The ipsilateral IC, which demonstrated few changes 2-days post exposure, underwent a massive downregulation of 73 of 84 synaptic plasticity genes at 28-d post-exposure (Figure 2C). There were no significant increases in gene expression at 28-d post-exposure consistent with the 2-d post-exposure data. The 73 genes significantly downregulated are shown in bold text in Table 5 and as blue symbols in the volcano plot of Figure 2C. The two genes that were downregulated at 2-d post-exposure, *Ngfr* and *Tnf*, were downregulated even further at 28-d post-exposure. The numbers of downregulated genes in the 10 gene categories (Table 2) were: 21 in LTD, 22 in LTP, 22 in IEG, 2 in LRG, 9 in CA, 4 in EMP, 9 in CC, 18 in NR, 15 in PSD and 2 in OT. Thus, most of the genes in all 10 categories were downregulated.

Gene Expression Changes in Contralateral IC 28-d Post-Exposure: The 28-d post-exposure gene expression data for the contralateral IC are presented in Figure 2D and Table 6. Substantially fewer synaptic plasticity genes were downregulated at 28-d post-exposure than at 2-d post-exposure; no genes were upregulated at this time. Among the 84 synaptic plasticity genes, only 12 were significantly downregulated 28-d post-exposure. Most of the genes that

13

had been significantly downregulated in the contralateral IC at 2-d post-exposure had recovered at 28-d post-exposure and were within the "normal" range (less than 50% increase or decrease). However, 12 of the genes that were significantly downregulated at 2-d post-exposure (*Arc, Cebpd, Egr1, Egr2, Egr3, Fos, Grin2c, Junb, Ngfr, Nr4a1, Pim 1 and Tnf*) were still significantly downregulated at 28-d post-exposure. The numbers of downregulated genes in each of the 10 categories (Table 2) were: 1 in LTD, 1 in LTP, 8 in IEG, 0 in LRG, 1 in CA, 0 in EMP, 1 in CC, 1 in NR, 2 in PSD and 0 in OT.

Gene Expression Shifts from Contralateral to Ipsilateral IC: To illustrate the dynamic changes in gene expression, Figure 3 plots the fold change of each gene at 28-d post-exposure versus its fold change 2-d post-exposure, i.e., late changes versus early changes. Points above the diagonal reflect an increase in gene expression from 2-d to 28-d post-exposure whereas points below the diagonal reflect time-dependent decreases. Points to the left of the dashed vertical blue line indicate fold decreases greater than 50% (FC<0.05) whereas points to the right of the dashed vertical red indicate fold increases greater than 50% (FC>1.5, red line out of range and absent in Figure 3B). Most of the fold change values in the ipsilateral IC were largely unchanged at 2-d post-exposure (i.e., value between 0.5 and 1.5). However, nearly all of the gene expression values in the ipsilateral IC had declined substantially at 28-d post-exposure and therefore were below the diagonal. By contrast, most of the values in the contralateral IC were already substantially reduced (i.e., <0.5) at 2-d post-exposure. However, most of the fold-change values had increased from 2-d to 28-d and so that the values were now above the diagonal and within the "normal" range, i.e., 0.5 to 1.5. Thus, the temporal dynamics of gene expression in the ipsilateral and contralateral IC were largely out of phase. There was a substantial decrease in gene expression in the ipsilateral IC between 2-d and 28-d post-exposure. By contrast, the gene expression changes were already substantially reduced in the contralateral IC at 2-d post-exposure but then largely recovered (increased) to the "normal" range by 28-d post-exposure.

14

Figure 4 illustrates the temporal fluctuation in gene expression within each of the 10 gene functional categories. To put the data into perspective, Figure 4A shows the percentage of synaptic plasticity genes within each of the 10 categories. The six categories with the highest representation were: 18% LTD, 18% IEG, 17% LTP, 12% NR, 9% PSD and 9% LRG. Each bar in the histograms shows the percentage of genes within each of the 10 categories that showed a statistically significant change in the ipsilateral and contralateral IC at 2-d post-exposure (Figure 4B) and 28-d post-exposure (Figure 4C). Only 2 genes declined significantly in the ipsilateral IC at 2-d post-exposure, one gene was in the LTD category and the other in CA group. By contrast, most of synaptic plasticity genes declined significantly in the contralateral IC 2-d post-exposure; 40% or more of the genes within each category had decreased significantly (Figure 4B). The 5 categories with the largest changes were: CA, OT, NR, PSD and LTD. At 28-d post-exposure, more than 75% of the genes within each of the 10 categories had decreased significantly in the ipsilateral IC (Figure 4C, blue bars). In contrast, only a small percentage of genes among the 10 categories were significantly downregulated in the contralateral IC at 28-d post-exposure (Figure 4C, red bars), most of the decreases were in the immediate early gene category.

mRNA in situ Hybridization: Gene array studies provide a global perspective of the noise-induced mRNA changes that occur in the brain. To confirm the general findings of the gene array studies, we localized mRNA expression in brain sections from the IC using a commercial RNA in situ hybridization kit (RNA-CISH) with appropriate controls. Because it was not practical to evaluate all genes that were differentially expressed in the ipsilateral and contralateral IC at 28 post-exposure time points, only two genes, *Egr1* and *Arc,* were evaluated based on the extent of noise-induced changes in gene expression, potential relevance to auditory synaptic plasticity, and availability of rat-specific probes. *Arc* was selected for RNA-CISH analysis because it showed a large 8-fold decrease on the ipsilateral side at 28-d post-exposure, that contrasted with a 3.7-fold decrease on the contralateral side at 28-d post-

15

exposure. In addition, we chose *Egr1* for RNA-CISH analysis because of the large 10-fold

decrease on the ipsilateral side at 28-d post-exposure contrasted with a 2.4-fold decrease on

the contralateral side at 28-d post-exposure. The purpose of these studies was to determine if

the decreases observed in the gene array studies were also reflected by a generalized

decrease in mRNA expression in the IC. We did not perform a comprehensive assessment of

the distribution of *Arc* and *Egr1* mRNA in the various cells types located throughout the IC.

Figure 5A-C contains representative photomicrographs of coronal sections from the

central nucleus of the IC showing *Arc* mRNA labeling; sections were obtained from unexposed

sham controls and from the ipsilateral and contralateral IC of noise-exposed rats sacrificed 28-d

post-exposure. The sections were counterstained with Gills hematoxylin to label nuclei and the

cell soma. In the sham controls, numerous reddish puncta were present bilaterally in large,

dense clusters around the cell body together with smaller, scattered puncta (Figure 5A). At 28-d

post-exposure, only small, scattered puncta of *Arc* mRNA labeling was evident in the ipsilateral

IC (Figure 5B). As illustrated by the results in this photomicrograph, *Arc* mRNA labeling was

greatly reduced consistent with the large decrease in *Arc* gene expression. In the contralateral

IC, some moderately intense reddish clusters of *Arc* mRNA were present with small, scattered

puncta (Figure 5C). *Arc* mRNA labeling in the contralateral IC was slightly greater than in the

ipsilateral IC consistent with gene array analysis. While there were regional variations in *Arc*

mRNA.

Figure 5D-F presents representative sections illustrating *Egr1* mRNA labeling in the

central nucleus of the IC from sham controls and from the ipsilateral and contralateral IC at 28-d

post-exposure. Many large, dense reddish *Egr1* labeled puncta were present around the cell

bodies. (Figure 5D). At 28-d post-exposure, *Egr1* mRNA labeling intensity was greatly reduced

in the ipsilateral IC (Figure 5B), consistent with the large decrease in *Egr1* gene expression. In

the contralateral IC, some moderately intense reddish clusters of *Egr1* mRNA labeling were

present around some cell bodies (Figure 5E). *Egr1* mRNA labeling in the contralateral IC was

16

slightly greater than on the ipsilateral side. Figure 5G shows results with the positive ubiquitin (*Ubc*) control probe (ubiquitin), with red puncta throughout the tissue, but with less intensity than *Egr* or *Arc*, a consequence of it widespread, but lower intense labeling.

Discussion

  IC Synaptic Plasticity Gene Profile: *Rab3a*, the most abundant synaptic plasticity gene in our sample from the IC, encodes the Ras-related protein Rab-3A involved in calcium mediated exocytosis, an important process in neurotransmitter release (Geppert et al., 1994). *Gria2*, the second most abundant gene in the IC, encodes the excitatory glutamate ionotropic AMPA receptor subunit 2, suggesting that this particular receptor plays an important role in excitatory neurotransmission in the IC (Chen et al., 2001). Ppp3ca, the third most abundant gene, codes for subunits of calcineurin A, a protein involved in the transduction of intracellular calcium-mediated signals (Wang et al., 1996). Calcineurin A alpha isozyme mRNAs are expressed at relatively high levels in the IC (Buttini et al., 1993) where it could play a key role in activity dependent modulation of inhibitory neurotransmission (Bannai et al., 2009). *Mapk1*, the fourth most abundant IC synaptic plasticity gene, codes for mitogen-activate protein kinase 1 (also known as ERK2), involved in proliferation, differentiation and transcription. Dynamic changes in phosphorylated ERK2 in the IC following unilateral cochlear ablation (Suneja and Potashner, 2003) could contribute to the growth and rearrangement of synapse, changes in neurotransmitter release, heightened spontaneous activity and enhanced sound-evoked neural activity (Benson et al., 1997, Suneja et al., 1998, Salvi et al., 2000, Mulders and Robertson, 2009). *Ywhaq,* the fifth most abundant synaptic plasticity gene, codes a family of 14-3-3 proteins involved in signal transduction, apoptosis and proliferation (Malaspina et al., 2000). *Ywhaq* has been implicated in synaptic remodeling in the IC and the formation of auditory space maps which are derived from neurons sensitive to IID and ITD (Swofford and DeBello, 2007). Noise-induced changes in *Ywhaq* expression could lead to remodeling of synapses of neurons sensitive to IID and ITD.

17

Eight of the 10 most abundantly expressed synaptic plasticity genes in the IC were also among the top 10 synaptic plasticity genes we observed in the VCN and/or DCN in our earlier study (Manohar et al., 2019). *Gria2*, which was among the top 10 most abundant genes in the IC; was also among the top 10 in the DCN. Seven of the other 10 most abundantly expressed synaptic plasticity genes in the IC, *Gnai1, Mapk1, Ntrk2, Ppp2ca, Rab3a, Rheb* and *Ywhaq*, were also in the top 10 in both the VCN and DCN. The two genes among the top 10 in the IC, Ppp1ca and Ppp3ca, were not in the top 10 in the DCN and VCN. Nevertheless, these two genes were expressed at similarly high levels in the cochlear nuclei. These results suggest that the genes important for synaptic plasticity in the IC are similar to those in the cochlear nuclei.

Severe Unilateral Noise-Induced Hearing Loss: The 126 dB exposure produced a severe hearing loss in the left ear without affecting the contralateral ear that was plugged and protected during the exposure. These results accord well with our previous studies showing that this exposure causes massive loss of both inner and outer hair cells over nearly the entire length of the cochlea in all the noise-exposed ears without damaging hair cells in the contralateral cochlea (Kraus et al., 2010, Baizer et al., 2015). Because the IC receives afferent inputs from virtually all auditory nuclei on the contralateral and ipsilateral side of brainstem (Aitkin and Phillips, 1984b, Moore et al., 1998), we expected that the unilateral hearing loss would alter the expression of genes in both the ipsilateral and contralateral IC. However, it was unclear when these changes would occur on the ipsilateral and contralateral side, what genes would be affected, if mRNA levels would increase and/or decrease and if the changes would persist or recover. Although the traumatic noise exposure lasted only 2 h, a punctate event, the consequences of this peripheral damage on the central auditory were persistent and progressive as reflected by the fact that auditory nerve degeneration and microglia activation continued to occur in the cochlear nuclei for six months or more (Baizer et al., 2015). Therefore, dynamic changes in synaptic plasticity gene expression in the IC might be expected to occur over many months as neural circuits at lower and higher levels of the central nervous system

18

reorganize to compensate for the unilateral hearing loss and progressive degeneration of the auditory nerve fibers that innervate the cochlear nuclei (Illing, 2001, Illing et al., 2005, Kraus et al., 2009, Kraus et al., 2011). While many of the noise-induced changes in gene expression in the IC likely arise from a reduction of afferent inputs from more peripheral parts of the auditory pathway, some could result from altered signaling from descending projections from the auditory cortex and medial geniculate body (Adams, 1980, Winer et al., 1998, Mellott et al., 2014). Consistent with view, significant changes in gene expression were observed in the IC after lesions of the auditory cortex (Clarkson et al., 2012).

IC versus DCN and VCN 2-d Post-Exposure: We previously evaluated the changes in synaptic plasticity gene expression in the ipsilateral DCN and VCN 2-d following the same noise exposure employed in the current study (Manohar et al., 2019). Synaptic plasticity gene expression was not significantly altered in the DCN 2-d post-exposure; however, six genes in the ipsilateral VCN, *Bdnf, Cebpb, Crem, Egr1, Homer1* and *Pcdh8,* were significantly downregulated in the VCN. None of these six downregulated genes in the VCN overlapped with the two genes in the ipsilateral IC, *Ngfr* and *Tnf*, that were downregulated 2-d post-exposure. Tnf encodes for TNF, a proinflammatory cytokine mainly secreted by brain microglia and astrocytes. TNF-alpha can profoundly alter neural activity by potentiating excitatory neurotransmission while downregulating inhibitory neurotransmission (Stellwagen et al., 2005, Santello and Volterra, 2012, Olmos and Llado, 2014). However, five of the six genes downregulated in the ipsilateral VCN 2-d post-exposure, *Bdnf, Cebpb, Egr1, Homer1* and *Pcdh8,* were also significantly downregulated in the contralateral IC at this time. One surprising difference between the IC and VCN was the number of genes that were downregulated at 2-d post-exposure. Only 6 of 84 genes were downregulated in the ipsilateral VCN 2-d post-exposure whereas 65 of 84 genes were downregulated in the IC. Thus, the gene expression downregulation in the contralateral IC was much more widespread and substantial greater than

in either the VCN or DCN 2-post-exposure, an interesting result given that the IC is further removed from the cochlear lesion than the VCN and DCN.

Early Gene Expression Changes: Most of the synaptic plasticity genes were downregulated after the noise exposure, while none were upregulated. This downward trend is consistent with previous reports showing a general decline in mRNAs encoding excitatory and inhibitory proteins in the IC immediately following noise-induced temporary threshold shift (Dong et al., 2010a) or unilateral cochlear damage (Dong et al., 2009). While gene expression was generally decreased immediately after noise-induced temporary threshold shift, the expression of many of the downregulated genes returned to near normal levels or in some cases were over expressed two- and four-weeks post-exposure presumably due to the fact that the cochlear hearing loss had nearly recovered by four-weeks post-exposure (Dong et al., 2010a). These results contrast markedly with the large, persistent threshold shift (Figure 1) and hair cell loss that resulted from our 126 dB exposure (Baizer et al., 2015).

The initial downregulation at 2-d post-exposure affected many genes in the contralateral IC, whereas only a few decreases were observed in the ipsilateral IC (Figure 2A-B). This early downregulation in the contralateral IC could be related to the fact that sounds delivered to the ipsilateral ear evoke more robust and shorter latency responses in the contralateral IC (Semple and Kitzes, 1985, Popelar et al., 1994, McAlpine et al., 1997). The contralateral IC also receives many ascending inputs from the ipsilateral cochlear nucleus on the side with the noise-damaged cochlea (Adams, 1979, Nordeen et al., 1983). The prominent connectivity of the contralateral IC with the noise-damaged cochlear may contribute to the early changes in the contralateral IC.

At 2-d post-exposure, 40% or more of the genes in all 10 gene categories were significantly depressed in the contralateral IC (Figure 4B). The categories in which a large percentage of genes were downregulated included long-term depression, cell adhesion and neuronal receptors and postsynaptic density. Cell adhesion molecules, which bring pre- and

post-synaptic cells into contact, play an important role in many different aspects of synaptic function (Thalhammer and Cingolani, 2014). Decreased expression of genes involved in cell adhesion such as *Adam10, Cdh2, Ncam1 and Pcdh8* could lead to the uncoupling of synaptic connections in the IC due to the loss of neural activity from the noise-damaged cochlea. The reduced expression of *Adam10*, which encodes the metalloproteinase Adam10, could conceivably reduce the number of dendritic spines and degrade glutamatergic synaptic transmission (Marcello et al., 2017). Similarly, the noise-induced downregulation of *Cdh2,* which codes for N-cadherin, could suppress neurite branching shortly after the noise trauma (Yamagata et al., 2018).

IC vs DCN and VCN 28-d Post-Exposure: The changes in IC synaptic plasticity gene expression can be compare to those seen in the ipsilateral DCN and VCN 28-d following the same noise exposure employed in this study (Manohar et al., 2019). At 28-d post-exposure, the expression levels of two genes, *Ntf3* and *Ntf4*, were significantly upregulated in the ipsilateral DCN. In contrast, the expression level of Ntf3 was downregulated in the ipsilateral IC. In the ipsilateral VCN, the expression levels of 62 of 84 genes were significantly downregulated whereas 73 were significantly downregulated in the ipsilateral IC; most of the genes downregulated in ipsilateral VCN were also downregulated in the IC. Thus, the gene expression downregulation in the ipsilateral VCN appeared to be largely consistent with those in the ipsilateral IC. In contrast, the expression levels of only12 genes were significantly downregulated in the contralateral IC; among these, only 6, *Arc, Egr1, Fos, Grin2c, Junb* and *Pim1*, were also downregulated in the ipsilateral VCN.

Contralateral Recovery of Gene Expression Changes: Most of the 65 plasticity genes in the contralateral IC that were significantly downregulated at 2-d post-exposure had recovered by 28-d post-exposure (Figure 2B, D and 3B), while only a small percentage were still significantly downregulated. There was substantial recovery among the genes involved in long-term depression, long-term potentiation, cell adhesion, neuronal receptors and postsynaptic

density (Figure 4B vs. 4C). Some genes that partially or completely recovered at 28-d post-exposure included glutamate metabotropic receptors (Grm1, Grm2, Grm3, Grm4, Grm5, Grm7, Grm8), glutamate ionotropic NMDA receptors (*Grin2a, Grin2b, Grin2d)* and ionotropic AMPA receptors (Gria1, Gria2, Gria3, Gria4); these genes are associated with the long-term depression, long-term potentiation, neuronal receptors and postsynaptic density proteins (Table 2, 4, 6). The recovery of these genes, which regulate glutamatergic synaptic function and excitability, could contribute to the gradual buildup of spontaneous activity in the contralateral IC following unilateral NIHL (Sotgiu et al., 2003, Mulders and Robertson, 2009, Manzoor et al., 2012, Milanese et al., 2014, Naydenov et al., 2014, David-Pereira et al., 2017). The increased expression of glutamatergic genes might also be linked to GAP-43, a protein involved in axonal outgrowth and synaptic plasticity that is upregulated in the contralateral and ipsilateral IC after unilateral NIHL (Brainard and Knudsen, 1995, Michler and Illing, 2002). This interpretation is consistent with studies showing that glutamate agonists increase GAP-43 mRNA expression whereas glutamate antagonists decrease its expression (Console-Bram et al., 1998).

IEG are expected to show an acute increase in expression followed by a decline within a few hours. However, in our study, the expression levels of IEG in the IC were always downregulated, never upregulated above baseline levels. Among the genes in the "early responder" category that remained significantly downregulated in the contralateral IC at 28-d post-exposure were *Fos, Egr1, Egr2*, *Egr3*, and *Arc*, *Junb* and *Pim1* and growth factor-related genes *Tnf and Ngfr*. The persistent downregulation of these IEG at 28-d post-exposure suggests that the synaptic response to noise exposure is an ongoing and evolving process. One factor likely to contribute to the persistent decrease of these immediate early gene in the prolonged period (>6 months) of auditory nerve fibers degeneration which is accompanied by prolonged upregulation of microglia in the cochlear nucleus (Baizer et al., 2015). Consistent with the gene array data, *Arc* and *Egr1* were also downregulated with RNA-CISH (Figure 5). The *Egr* genes, which codes for early growth response proteins, are transcriptional regulators

whose gene products contribute to differentiation and neuroplasticity (Knapska and Kaczmarek, 2004). *Arc* and its protein product are involved in long-term potentiation, depression and homeostatic plasticity (Epstein and Finkbeiner, 2018). Both *Arc* and *Egr1*, activated by the mitogen-activated protein (MAP) kinase pathway (Davis et al., 2000, Waltereit et al., 2001), are also downregulated in the IC after acute and chronic treatment with sodium salicylate, which induces temporary cochlear hearing loss (Hu et al., 2014). *Arc* and other *Egr* genes are also decreased in the auditory cortex 2-weeks after bilateral cochlear ablation, but these genes largely recovered by 4-weeks post-ablation (Oh et al., 2007).

Delayed Downregulation in Ipsilateral IC: Surprisingly, there was a delayed, but massive downregulation of synaptic plasticity genes in the ipsilateral IC at 28-d post-exposure. More than 75% of the synaptic plasticity genes had decreased significantly in the ipsilateral IC whereas many genes in the contralateral IC were trending back toward to pre-exposure levels. Interestingly, many of the genes downregulated in the ipsilateral IC 28-d post exposure were the same ones that decreased significantly in the VCN 1-month post-exposure (Manohar et al., 2019).

The mechanisms responsible for the delayed downregulation in the ipsilateral IC are poorly understood. One possibility is that changes in the ipsilateral IC at 28-d post-exposure are triggered by the earlier changes in the contralateral IC, which are in turn relayed to the ipsilateral IC through inter-commissural connections (Aitkin and Phillips, 1984a, Coleman and Clerici, 1987, Gonzalez-Hernandez et al., 1996). One phenomenon related to these delayed gene expression changes is that the ipsilateral IC normally responds more weakly to ipsilateral than contralateral sound stimulation (Popelar et al., 1994). However, a few weeks after destruction of the contralateral cochlea, the ipsilateral IC gradually begins to respond more robustly to ipsilateral sound stimulation.

Another factor that could contribute to the delayed gene expression changes in the ipsilateral IC as well as the contralateral IC is neural cell loss observed in the IC and well as

other auditory nuclei following noise-induced permanent threshold shift (Groschel et al., 2010). Cell loss in the IC and other central auditory structures could be mediated in part by upregulation and downregulation of pro-apoptotic and anti-apoptotic genes and proteins in studies of acute and permanent noise-induced hearing loss (Groschel et al., 2018).

Except for *Grm8*, all the genes downregulated in the ipsilateral IC at 28-d post-exposure were the same ones that had previously been downregulated in the contralateral IC at 2-d post-exposure (Table 4-5). Thus, the downregulation seen in the ipsilateral IC 28-d post-exposure seemed to largely recapitulate the changes seen in the contralateral IC at 2-d post-exposure. However, eight additional genes (*Grin1, Nfkbib, Ppp1r14a, Ppp3ca, Rab3a, Synpo, Timp1* and *Ywhaq*) were also significantly downregulated in the ipsilateral IC at 28-d post exposure. Many of these were in the LTP category (*Grin1, Ppp3ca, Rab3a and Ywhaq*). Others have reported decreased expression of *Rab3a* in the contralateral IC 1-week after inducing a high-frequency cochlear lesion (Dong et al., 2009); this decrease was associated with increased spontaneous rates among high-frequency neurons in the contralateral IC. Decreased expression of *Rab3a* and *Ppp1r14a* have has also been observed in the ventral cochlear nucleus 28-d post-noise exposure (Manohar et al., 2019). Elimination of the Rab-3a protein in the hippocampus of knockout mice abolishes LTP (Castillo et al., 1997) and increases synaptic depression in the hippocampus after high-frequency pulse trains (Geppert et al., 1994). Such changes in Rab-3a mediated synaptic function could disrupt ITD processing and auditory temporal processing in the IC of subjects with cochlear hearing loss. Similarly, a significant decrease *Grin1* (glutamate ionotropic NMDA receptor) was seen in the IC of C57 mice with high-frequency age-related hearing loss (Osumi et al., 2012). Grin1, which codes for the glutamate NMDAR1 receptor subunit, is thought to play an important role in neuroplasticity. NMDAR1 knockout mice show increased pyramidal cell excitability in forebrain neurons because of altered membrane properties (Tatard-Leitman et al., 2015). Mice with high-frequency age-related hearing loss show behavioral and electrophysiological evidence of hyperactivity to suprathreshold low-

frequency stimuli (Willott and Turner, 2000). Similarly, high-frequency noise-induced hearing

loss leads to sound-evoked hyperactivity to low-frequency sounds in the IC (Salvi et al., 1990).

Unresponsive Genes: While the expression level of many genes changed significantly,

9 genes were unresponsive to unilateral hearing loss; their values did not change significantly in

the ipsilateral or contralateral IC at 2-d or 28-d post-exposure. Four of the unresponsive genes,

Crem, Egr4, Ngf and *Rheb*, were in the immediate early gene category. Excessive stimulation

of dopamine receptors in the striatum increases the expression of *Crem* (Berke et al., 1998).

Spinal cord lesions upregulate the expression of *Ngf* mRNA near the lesion, but not at sites

distant from the lesion which may explain the lack of change in the IC (Brown et al., 2007). The

other five unresponsive genes, *Igf1, Mapk1, Mmp9, Ntf4* and *Prkg1*, were in the LTP and/or LTD

categories. Lesions of the hippocampal dentate gyrus resulted in increased expression in *Igf1*

mRNA in microglia within the lesioned area (Breese et al., 1996). We have found that intense

noise exposure activates microglia in the cochlear nucleus (Baizer et al., 2015). However, we

have not observed microglia activation in the IC after unilateral NIHL (unpublished data), which

may explain why *Igf1* expression was unchanged in the IC.

Synopsis: Unilateral hearing loss disrupts many aspects of auditory perception,

especially those that require the integration of acoustic cues derived from both ears (Hawkins et

al., 1987, Firszt et al., 2017, Agterberg et al., 2019). Not surprisingly, when one ear is severely

damaged, the functional properties of IC neurons are altered as a result of the lack of sensory

input and the resulting neurodegenerative and neuroplastic changes in the central auditory

pathway and elsewhere in the central nervous system (Moore and Irvine, 1981, Popelar et al.,

1994, Kim et al., 1997, McAlpine et al., 1997, Morest et al., 1997). Compensatory neuroplastic

changes occurring in the IC could lead to the loss, rearrangement and modification of the

synaptic machinery within the IC (Suneja et al., 2000, Suneja and Potashner, 2003, Mo et al.,

2006). Most synaptic plasticity genes, which regulate neural activity, were significantly

downregulated in the contralateral IC 2-d post-exposure. The expression levels of most of the

downregulated genes had largely recovered to baseline levels by 28-d post-exposure.

Surprisingly, very few synaptic plasticity genes were downregulated in the ipsilateral IC 2-d

post-exposure. However, this was followed by a massive downregulation of more than 75% of

the synaptic plasticity genes in the ipsilateral IC at 28-d post-exposure. The location and time

course of these gene expression changes in the ipsilateral and contralateral IC provide

important new clues regarding the molecular and genetic changes that modulate the structural

and functional changes that occur in the IC following severe unilateral NIHL. The noise-induced

hearing loss genes that we identified in the IC represent potential therapeutic targets for treating

the phantom sound of tinnitus and improving the perceptual outcomes in patients with a

cochlear implant.

References

Adams JC (1979) Ascending projections to the inferior colliculus. J Comp Neurol 183:519-538.

Adams JC (1980) Crossed and descending projections to the inferior colliculus. Neurosci Lett 19:1-5.

Agterberg MJH, Snik AFM, Van de Goor RMG, Hol MKS, Van Opstal AJ (2019) Sound-localization performance of patients with single-sided deafness is not improved when listening with a bone-conduction device. Hear Res 372:62-68.

Aitkin LM, Dickhaus H, Schult W, Zimmermann M (1978) External nucleus of inferior colliculus: auditory and spinal somatosensory afferents and their interactions. J Neurophysiol 41:837-847.

Aitkin LM, Phillips SC (1984a) The Interconnections of the Inferior Colliculi through Their Commissure. Journal of Comparative Neurology 228:210-216.

Aitkin LM, Phillips SC (1984b) Is the Inferior Colliculus an Obligatory Relay in the Cat Auditory-System. Neurosci Lett 44:259-264.

Baizer JS, Wong KM, Manohar S, Hayes SH, Ding D, Dingman R, Salvi RJ (2015) Effects of acoustic trauma on the auditory system of the rat: The role of microglia. Neuroscience 303:299-311.

Bannai H, Levi S, Schweizer C, Inoue T, Launey T, Racine V, Sibarita JB, Mikoshiba K, Triller A (2009) Activity-dependent tuning of inhibitory neurotransmission based on GABAAR diffusion dynamics. Neuron 62:670-682.

Benson CG, Gross JS, Suneja SK, Potashner SJ (1997) Synaptophysin immunoreactivity in the cochlear nucleus after unilateral cochlear or ossicular removal. Synapse 25:243-257.

Berke JD, Paletzki RF, Aronson GJ, Hyman SE, Gerfen CR (1998) A complex program of striatal gene expression induced by dopaminergic stimulation. J Neurosci 18:5301-5310.

Blauert J (1983) Spatial hearing: the psychophyics of human sound localiation. Cambridge, MA: MIT Press.

Brainard MS, Knudsen EI (1995) Dynamics of visually guided auditory plasticity in the optic tectum of the barn owl. J Neurophysiol 73:595-614.

Breese CR, D'Costa A, Rollins YD, Adams C, Booze RM, Sonntag WE, Leonard S (1996) Expression of insulin-like growth factor-1 (IGF-1) and IGF-binding protein 2 (IGF-BP2) in the hippocampus following cytotoxic lesion of the dentate gyrus. J Comp Neurol 369:388-404.

Broudy VC, Harlan JM, Adamson JW (1987) Disparate effects of tumor necrosis factor-alpha/cachectin and tumor necrosis factor-beta/lymphotoxin on hematopoietic growth factor production and neutrophil adhesion molecule expression by cultured human endothelial cells. J Immunol 138:4298-4302.

Brown A, Ricci MJ, Weaver LC (2007) NGF mRNA is expressed in the dorsal root ganglia after spinal cord injury in the rat. Exp Neurol 205:283-286.

Buttini M, Limonta S, Luyten M, Boddeke H (1993) Differential distribution of calcineurin A alpha isoenzyme mRNA's in rat brain. Naunyn Schmiedebergs Arch Pharmacol 348:679-683.

Castillo PE, Janz R, Sudhof TC, Tzounopoulos T, Malenka RC, Nicoll RA (1997) Rab3A is essential for mossy fibre long-term potentiation in the hippocampus. Nature 388:590-593.

Chen GD, Decker B, Krishnan Muthaiah VP, Sheppard A, Salvi R (2014) Prolonged noise exposure-induced auditory threshold shifts in rats. Hear Res 317:1-8.

Chen GD, Kermany MH, D'Elia A, Ralli M, Tanaka C, Bielefeld EC, Ding D, Henderson D, Salvi R (2010) Too much of a good thing: long-term treatment with salicylate strengthens outer hair cell function but impairs auditory neural activity. Hear Res 265:63-69.

Chen YC, Kung SS, Chen BY, Hung CC, Chen CC, Wang TY, Wu YM, Lin WH, Tzeng CS, Chow WY (2001) Identifications, classification, and evolution of the vertebrate alpha-amino-3-hydroxy-5-methyl-4-isoxazole propionic acid (AMPA) receptor subunit genes. J Mol Evol 53:690-702.

28

Clarkson C, Herrero-Turrion MJ, Merchan MA (2012) Cortical Auditory Deafferentation Induces Long-Term Plasticity in the Inferior Colliculus of Adult Rats: Microarray and qPCR Analysis. Front Neural Circuits 6:86.

Coleman JR, Clerici WJ (1987) Sources of projections to subdivisions of the inferior colliculus in the rat. J Comp Neurol 262:215-226.

Console-Bram LM, Baird DH, Fitzpatrick-McElligott SG, McElligott JG (1998) Modulation of GAP-43 mRNA by GABA and glutamate in cultured cerebellar granule cells. Brain research 783:316-325.

Cox RA, Anders GT, Cappelli PJ, Johnson JE, Blanton HM, Seaworth BJ, Treasure RL (1990) Production of tumor necrosis factor-alpha and interleukin-1 by alveolar macrophages from HIV-1-infected persons. AIDS Res Hum Retroviruses 6:431-441.

David-Pereira A, Sagalajev B, Wei H, Almeida A, Pertovaara A, Pinto-Ribeiro F (2017) The medullary dorsal reticular nucleus as a relay for descending pronociception induced by the mGluR5 in the rat infralimbic cortex. Neuroscience 349:341-354.

Davis S, Vanhoutte P, Pages C, Caboche J, Laroche S (2000) The MAPK/ERK cascade targets both Elk-1 and cAMP response element-binding protein to control long-term potentiation-dependent gene expression in the dentate gyrus in vivo. J Neurosci 20:4563-4572.

Dong S, Mulders WH, Rodger J, Robertson D (2009) Changes in neuronal activity and gene expression in guinea-pig auditory brainstem after unilateral partial hearing loss. Neuroscience 159:1164-1174.

Dong S, Mulders WH, Rodger J, Woo S, Robertson D (2010a) Acoustic trauma evokes hyperactivity and changes in gene expression in guinea-pig auditory brainstem. Eur J Neurosci 31:1616-1628.

Dong S, Rodger J, Mulders WH, Robertson D (2010b) Tonotopic changes in GABA receptor expression in guinea pig inferior colliculus after partial unilateral hearing loss. Brain research 1342:24-32.

Epstein I, Finkbeiner S (2018) The Arc of cognition: Signaling cascades regulating Arc and implications for cognitive function and disease. Semin Cell Dev Biol 77:63-72.

Firszt JB, Reeder RM, Holden LK (2017) Unilateral Hearing Loss: Understanding Speech Recognition and Localization Variability-Implications for Cochlear Implant Candidacy. Ear Hear 38:159-173.

Geppert M, Bolshakov VY, Siegelbaum SA, Takei K, De Camilli P, Hammer RE, Sudhof TC (1994) The role of Rab3A in neurotransmitter release. Nature 369:493-497.

Gonzalez-Hernandez T, Mantolan-Sarmiento B, Gonzalez-Gonzalez B, Perez-Gonzalez H (1996) Sources of GABAergic input to the inferior colliculus of the rat. J Comp Neurol 372:309-326.

Groschel M, Basta D, Ernst A, Mazurek B, Szczepek AJ (2018) Acute Noise Exposure Is Associated With Intrinsic Apoptosis in Murine Central Auditory Pathway. Front Neurosci 12:312.

Groschel M, Gotze R, Ernst A, Basta D (2010) Differential impact of temporary and permanent noise-induced hearing loss on neuronal cell density in the mouse central auditory pathway. J Neurotrauma 27:1499-1507.

Hawkins DB, Prosek RA, Walden BE, Montgomery AA (1987) Binaural loudness summation in the hearing impaired. J Speech Hear Res 30:37-43.

Heffner HE, Harrington IA (2002) Tinnitus in hamsters following exposure to intense sound. Hear Res 170:83-95.

Horvath D, Lesica NA (2011) The effects of interaural time difference and intensity on the coding of low-frequency sounds in the mammalian midbrain. J Neurosci 31:3821-3827.

Hu BH, Cai Q, Manohar S, Jiang H, Ding D, Coling DE, Zheng G, Salvi R (2009) Differential expression of apoptosis-related genes in the cochlea of noise-exposed rats. Neuroscience 161:915-925.

Hu SS, Mei L, Chen JY, Huang ZW, Wu H (2014) Expression of immediate-early genes in the inferior colliculus and auditory cortex in salicylate-induced tinnitus in rat. Eur J Histochem 58:2294.

Humes L, Joellenbeck LM, Durch J, Institute of Medicine (U.S.). Committee on Noise-Induced Hearing Loss and Tinnitus Associated with Military Service from World War II to the Present. (2006) Noise and military service : implications for hearing loss and tinnitus. Washington, DC: National Academies Press.

Illing RB (2001) Activity-dependent plasticity in the adult auditory brainstem. Audiology & neuro-otology 6:319-345.

Illing RB, Kraus KS, Meidinger MA (2005) Reconnecting neuronal networks in the auditory brainstem following unilateral deafening. Hear Res 206:185-199.

Jamesdaniel S, Ding D, Kermany MH, Davidson BA, Knight PR, 3rd, Salvi R, Coling DE (2008) Proteomic analysis of the balance between survival and cell death responses in cisplatin-mediated ototoxicity. J Proteome Res 7:3516-3524.

Kim J, Morest DK, Bohne BA (1997) Degeneration of axons in the brainstem of the chinchilla after auditory overstimulation. Hear Res 103:169-191.

Knapska E, Kaczmarek L (2004) A gene for neuronal plasticity in the mammalian brain: Zif268/Egr-1/NGFI-A/Krox-24/TIS8/ZENK? Prog Neurobiol 74:183-211.

Kraus KS, Ding D, Jiang H, Lobarinas E, Sun W, Salvi RJ (2011) Relationship between noise-induced hearing-loss, persistent tinnitus and growth-associated protein-43 expression in the rat cochlear nucleus: does synaptic plasticity in ventral cochlear nucleus suppress tinnitus? Neuroscience 194:309-325.

Kraus KS, Ding D, Zhou Y, Salvi RJ (2009) Central auditory plasticity after carboplatin-induced unilateral inner ear damage in the chinchilla: up-regulation of GAP-43 in the ventral cochlear nucleus. Hear Res 255:33-43.

Kraus KS, Mitra S, Jimenez Z, Hinduja S, Ding D, Jiang H, Gray L, Lobarinas E, Sun W, Salvi RJ (2010) Noise trauma impairs neurogenesis in the rat hippocampus. Neuroscience 167:1216-1226.

Li L, Kelly JB (1992) Binaural responses in rat inferior colliculus following kainic acid lesions of the superior olive: interaural intensity difference functions. Hear Res 61:73-85.

Lim JC, Lu W, Beckel JM, Mitchell CH (2016) Neuronal Release of Cytokine IL-3 Triggered by Mechanosensitive Autostimulation of the P2X7 Receptor Is Neuroprotective. Front Cell Neurosci 10:270.

Liu H, Ding D, Jiang H, Wu X, Salvi R, Sun H (2011) Ototoxic destruction by co-administration of kanamycin and ethacrynic acid in rats. Biomed Biotechnol 12:85-61.

Ma WL, Hidaka H, May BJ (2006) Spontaneous activity in the inferior colliculus of CBA/J mice after manipulations that induce tinnitus. Hear Res 212:9-21.

Malaspina A, Kaushik N, de Belleroche J (2000) A 14-3-3 mRNA is up-regulated in amyotrophic lateral sclerosis spinal cord. J Neurochem 75:2511-2520.

Manohar S, Dahar K, Adler HJ, Dalian D, Salvi R (2016) Noise-induced hearing loss: Neuropathic pain via Ntrk1 signaling. Mol Cell Neurosci 75:101-112.

Manohar S, Jamesdaniel S, Salvi R (2014) Cisplatin inhibits hippocampal cell proliferation and alters the expression of apoptotic genes. Neurotox Res 25:369-380.

Manohar S, Ramchander PV, Salvi R, Seigel GM (2019) Synaptic Reorganization Response in the Cochlear Nucleus Following Intense Noise Exposure. Neuroscience 399:184-198.

Manzoor NF, Licari FG, Klapchar M, Elkin RL, Gao Y, Chen G, Kaltenbach JA (2012) Noise-induced hyperactivity in the inferior colliculus: its relationship with hyperactivity in the dorsal cochlear nucleus. J Neurophysiol 108:976-988.

Marcello E, Borroni B, Pelucchi S, Gardoni F, Di Luca M (2017) ADAM10 as a therapeutic target for brain diseases: from developmental disorders to Alzheimer's disease. Expert Opin Ther Targets 21:1017-1026.

McAlpine D, Martin RL, Mossop JE, Moore DR (1997) Response properties of neurons in the inferior colliculus of the monaurally deafened ferret to acoustic stimulation of the intact ear. J Neurophysiol 78:767-779.

Mellott JG, Bickford ME, Schofield BR (2014) Descending projections from auditory cortex to excitatory and inhibitory cells in the nucleus of the brachium of the inferior colliculus. Front Syst Neurosci 8:188.

Michler SA, Illing RB (2002) Acoustic trauma induces reemergence of the growth- and plasticity-associated protein GAP-43 in the rat auditory brainstem. J Comp Neurol 451:250-266.

Milanese M, Giribaldi F, Melone M, Bonifacino T, Musante I, Carminati E, Rossi PI, Vergani L, Voci A, Conti F, Puliti A, Bonanno G (2014) Knocking down metabotropic glutamate receptor 1 improves survival and disease progression in the SOD1(G93A) mouse model of amyotrophic lateral sclerosis. Neurobiol Dis 64:48-59.

Mo Z, Suneja SK, Potashner SJ (2006) Phosphorylated cAMP response element-binding protein levels in guinea pig brainstem auditory nuclei after unilateral cochlear ablation. J Neurosci Res 83:1323-1330.

Moon IS (2007) Noise-induced hearing loss caused by gunshot in South Korean military service. Mil Med 172:421-425.

Moore DR, Irvine DR (1981) Plasticity of binaural interaction in the cat inferior colliculus. Brain research 208:198-202.

Moore DR, Kotak VC, Sanes DH (1998) Commissural and lemniscal synaptic input to the gerbil inferior colliculus. J Neurophysiol 80:2229-2236.

Morest DK, Kim J, Bohne BA (1997) Neuronal and transneuronal degeneration of auditory axons in the brainstem after cochlear lesions in the chinchilla: cochleotopic and non-cochleotopic patterns. Hear Res 103:151-168.

Mulders WH, Robertson D (2009) Hyperactivity in the auditory midbrain after acoustic trauma: dependence on cochlear activity. Neuroscience 164:733-746.

Nakamoto KT, Shackleton TM, Magezi DA, Palmer AR (2015) A function for binaural integration in auditory grouping and segregation in the inferior colliculus. J Neurophysiol 113:1819-1830.

Naydenov AV, Sepers MD, Swinney K, Raymond LA, Palmiter RD, Stella N (2014) Genetic rescue of CB1 receptors on medium spiny neurons prevents loss of excitatory striatal synapses but not motor impairment in HD mice. Neurobiol Dis 71:140-150.

Nordeen KW, Killackey HP, Kitzes LM (1983) Ascending projections to the inferior colliculus following unilateral cochlear ablation in the neonatal gerbil, Meriones unguiculatus. J Comp Neurol 214:144-153.

Oh SH, Kim CS, Song JJ (2007) Gene expression and plasticity in the rat auditory cortex after bilateral cochlear ablation. Acta Otolaryngol 127:341-350.

Olmos G, Llado J (2014) Tumor necrosis factor alpha: a link between neuroinflammation and excitotoxicity. Mediators Inflamm 2014:861231.

Osumi Y, Shibata SB, Kanda S, Yagi M, Ooka H, Shimano T, Asako M, Kawamoto K, Kuriyama H, Inoue T, Nishiyama T, Yamashita T, Tomoda K (2012) Downregulation of N-methyl-D-aspartate receptor zeta1 subunit (GluN1) gene in inferior colliculus with aging. Brain research 1454:23-32.

Park TJ, Pollak GD (1993) GABA shapes sensitivity to interaural intensity disparities in the mustache bat's inferior colliculus: implications for encoding sound location. J Neurosci 13:2050-2067.

Popelar J, Erre JP, Aran JM, Cazals Y (1994) Plastic changes in ipsi-contralateral differences of auditory cortex and inferior colliculus evoked potentials after injury to one ear in the adult guinea pig. Hear Res 72:125-134.

Salvi RJ, Saunders SS, Gratton MA, Arehole S, Powers N (1990) Enhanced evoked response amplitudes in the inferior colliculus of the chinchilla following acoustic trauma. Hear Res 50:245-257.

Salvi RJ, Wang J, Ding D (2000) Auditory plasticity and hyperactivity following cochlear damage. Hear Res 147:261-274.

Santello M, Volterra A (2012) TNFalpha in synaptic function: switching gears. Trends in neurosciences 35:638-647.

Semple MN, Kitzes LM (1985) Single-unit responses in the inferior colliculus: different consequences of contralateral and ipsilateral auditory stimulation. J Neurophysiol 53:1467-1482.

Sotgiu ML, Bellomi P, Biella GE (2003) The mGluR5 selective antagonist 6-methyl-2-(phenylethynyl)-pyridine reduces the spinal neuron pain-related activity in mononeuropathic rats. Neurosci Lett 342:85-88.

Spongr V, Walton JP, Frisina RD, Kazee AM, Flood DG, Salvi RJ (1997) Hair cell loss and synaptic loss in inferior colliculus of C57BL/6 mice: Relationship to abnormal temporal processing. In: Auditory Signal Processing in the Central Auditory Pathway(Syka, J., ed), pp 535-542 New York.: Plenum Publishing Corp.

Stellwagen D, Beattie EC, Seo JY, Malenka RC (2005) Differential regulation of AMPA receptor and GABA receptor trafficking by tumor necrosis factor-alpha. J Neurosci 25:3219-3228.

Suneja SK, Potashner SJ (2003) ERK and SAPK signaling in auditory brainstem neurons after unilateral cochlear ablation. J Neurosci Res 73:235-245.

Suneja SK, Potashner SJ, Benson CG (1998) Plastic changes in glycine and GABA release and uptake in adult brain stem auditory nuclei after unilateral middle ear ossicle removal and cochlear ablation. Exp Neurol 151:273-288.

Suneja SK, Potashner SJ, Benson CG (2000) AMPA receptor binding in adult guinea pig brain stem auditory nuclei after unilateral cochlear ablation. Exp Neurol 165:355-369.

Swofford JA, DeBello WM (2007) Transcriptome changes associated with instructed learning in the barn owl auditory localization pathway. Dev Neurobiol 67:1457-1477.

35

Tatard-Leitman VM, Jutzeler CR, Suh J, Saunders JA, Billingslea EN, Morita S, White R, Featherstone RE, Ray R, Ortinski PI, Banerjee A, Gandal MJ, Lin R, Alexandrescu A, Liang Y, Gur RE, Borgmann-Winter KE, Carlson GC, Hahn CG, Siegel SJ (2015) Pyramidal cell selective ablation of N-methyl-D-aspartate receptor 1 causes increase in cellular and network excitability. Biol Psychiatry 77:556-568.

Thalhammer A, Cingolani LA (2014) Cell adhesion and homeostatic synaptic plasticity. Neuropharmacology 78:23-30.

Vogler DP, Robertson D, Mulders WH (2014) Hyperactivity following unilateral hearing loss in characterized cells in the inferior colliculus. Neuroscience 265C:28-36.

Waltereit R, Dammermann B, Wulff P, Scafidi J, Staubli U, Kauselmann G, Bundman M, Kuhl D (2001) Arg3.1/Arc mRNA induction by Ca2+ and cAMP requires protein kinase A and mitogen-activated protein kinase/extracellular regulated kinase activation. J Neurosci 21:5484-5493.

Walton JP, Frisina RD, O'Neill WE (1998) Age-related alteration in processing of temporal sound features in the auditory midbrain of the CBA mouse. J Neurosci 18:2764-2776.

Wang MG, Yi H, Guerini D, Klee CB, McBride OW (1996) Calcineurin A alpha (PPP3CA), calcineurin A beta (PPP3CB) and calcineurin B (PPP3R1) are located on human chromosomes 4, 10q21-->q22 and 2p16-->p15 respectively. Cytogenet Cell Genet 72:236-241.

Willott JF, Turner JG (2000) Neural plasticity in the mouse inferior colliculus: relationship to hearing loss, augmented acoustic stimulation, and prepulse inhibition. Hear Res 147:275-281.

Winer JA, Larue DT, Diehl JJ, Hefti BJ (1998) Auditory cortical projections to the cat inferior colliculus. J Comp Neurol 400:147-174.

Wu B, Eliscovich C, Yoon YJ, Singer RH (2016) Translation dynamics of single mRNAs in live cells and neurons. Science 352:1430-1435.

Wyatt S, Shooter EM, Davies AM (1990) Expression of the NGF receptor gene in sensory neurons and their cutaneous targets prior to and during innervation. Neuron 4:421-427.

Yamagata M, Duan X, Sanes JR (2018) Cadherins Interact With Synaptic Organizers to Promote Synaptic Differentiation. Front Mol Neurosci 11:142.

Yin TC, Chan JC (1990) Interaural time sensitivity in medial superior olive of cat. J Neurophysiol 64:465-488.

Figure Legends

Figure 1: Mean (+/- SD, n=3 per group) ABR thresholds measured from the left and right ear of the sham control group and the noise-exposed group (126 dB SPL, 2 h, 12 kHz narrow band noise) 28-d post-exposure. Right ear of noise-exposed group plugged during the exposure to prevent hearing loss in the right ear.

Figure 2: Volcano plots showing synaptic plasticity gene expression changes in the IC 2-d (top row) and 28-d (bottom row) post-exposure. Changes in the ipsilateral IC shown on the left (A, C) and changes in the contralateral IC shown on the right (B, C). Abscissa plots gene expression changes on Log_2 (fold change) format. Gene expression decreases greater than 50% represented by blue circles. Gene expression changes between -50% and +50% represented by open black circles. Ordinate show statistical significance plotted as $-Log_{10}$ (p value). Gene expression decreases >50% (left of the blue dashed line) and with p<0.5 (above green dashed line) were classified as significant changes in gene expression. None of the increases in gene expression exceeded +50%, therefore none of the increases were considered significant.

Figure 3: Scatterplot showing the fold change in synaptic plasticity genes expression at 28-d post-exposure versus fold change in gene expression 2-d post exposure for the (A) ipsilateral IC and (B) contralateral IC. Points above the diagonal line represent an increase in gene expression from 2-d to 28-d whereas points below the diagonal represent genes that decreased expression from 2-d to 28-d post-exposure. Most of the synaptic plasticity genes in the ipsilateral IC became downregulated 28-d post-exposure whereas most of the genes in the contralateral IC were already significantly downregulated (fold change <0.5) 2-d post-exposure, but the expression level of many of these genes had increased and had returned to the "normal" range (fold change greater than 0.5 and less than 1.5).

Figure 4: Synaptic plasticity gene expression firsts declined in IC contralateral to the noise-exposed followed several weeks later by a decline in the ipsilateral IC. (A) Pie chart showing the percentages of the synaptic plasticity genes in each of the 10 gene categories: LTD (long term depression), LTP (long term potentiation), IEG (immediate early gene), LRG (late response gene), CA (cell adhesion), EMP (extracellular matrix and proteolytic), CC (Creb cofactor), NR (neuronal receptor), PSD (postsynaptic density) and OT (other). (B) Percentage (%) of genes within each of the 10 categories that was significantly decreased at 2-d post-exposure in the ipsilateral IC (red) versus the IC contralateral to (blue dashed) the noise-exposed ear. At 2-d post-exposure, 40% or more of the genes in each of the 10 categories were depressed in the contralateral IC. (C) Percentage (%) genes within each of the 10 categories were significantly decreased at 28-d post-exposure in the ipsilateral IC (red) versus the IC contralateral to (blue dashed) the noise-exposed ear. At 28-d post-exposure, most of the genes in the 10 categories were depressed in the ipsilateral IC.

Figure 5: Representative photomicrographs of coronal sections from the ipsilateral and contralateral central nucleus of the inferior colliculus (IC); sections from sham controls (left) and those taken 28-d post-exposure from ipsilateral (middle row) or contralateral (right row) IC. Reddish puncta (arrows) show in situ labeling of mRNA probe for *Arc* (top row) and *Egr1* (bottom row). Sections counterstained with Gill's hematoxylin (blueish gray). Mean fold change (FC) in gene expression in controls and 28-d post-exposure groups shown in lower right of each panel. Many dark reddish puncta for *Arc* mRNA (A) and *Egr1* mRNA (D) around soma of cells from sham controls. Density and intensity of reddish puncta for *Arc* and *Egr1* greatly reduced in ipsilateral IC 28-d post-exposure (B and E) compared to labeling in unexposed sham control. Density and/or intensity of reddish puncta for Arc and Egr1 is greater in contralateral IC than in ipsilateral IC. Scale bar shown in panels A and D. Positive control probe for ubiquitin (*Ubc*) (G) shows widespread, but light reddish puncta for *Ubc* mRNA.

Highlights

- Intense unilateral noise exposure decreased IC synaptic plasticity gene expression

- Synaptic plasticity gene expression in ipsilateral IC largely unaltered 2d post-noise

- 65 of 84 synaptic plasticity gene levels decreased in contralateral IC 2d post-noise

- Most synaptic plasticity gene levels in contralateral IC recovered 28d post-noise

- 73 of 84 synaptic plasticity gene levels decreased in ipsilateral IC 28d post-exposure

- Complex spatio-temporal changes in IC gene expression post unilateral hearing loss

Table 1. Relative abundance (RA) of synaptic plasticity gene compared to actin. Top 10 most abundant genes in bold

Gene	RA	Gene	RA	Gene	RA
Adam10	0.043	Grin2a	0.021	Ntf3	0.001
Adcy1	0.003	Grin2b	0.019	Ntf4	0.000
Adcy8	0.017	Grin2c	0.000	**Ntrk2**	**0.094**
Akt1	0.019	Grin2d	0.003	Pcdh8	0.001
Arc	0.004	Grip1	0.003	Pick1	0.008
Bdnf	0.005	Grm1	0.004	Pim1	0.002
Camk2a	0.065	Grm2	0.001	Plat	0.030
Camk2g	0.058	Grm3	0.045	Plcg1	0.035
Cdh2	0.007	Grm4	0.006	**Ppp1ca**	**0.070**
Cebpb	0.000	Grm5	0.006	Ppp1cc	0.011
Cebpd	0.001	Grm7	0.016	Ppp1r14a	0.060
Cnr1	0.013	Grm8	0.007	**Ppp2ca**	**0.112**
Creb1	0.010	Homer1	0.027	**Ppp3ca**	**0.149**
Crem	0.008	Igf1	0.006	Prkca	0.027
Dlg4	0.029	Inhba	0.001	Prkcg	0.006
Egr1	0.007	Jun	0.023	Prkg1	0.005
Egr2	0.000	Junb	0.002	**Rab3a**	**0.418**
Egr3	0.003	Klf10	0.001	Rela	0.005
Egr4	0.001	**Mapk1**	**0.134**	Reln	0.030
Ephb2	0.002	Mmp9	0.000	RGD1562511	0.002

40

Fos	0.016	Ncam1	0.072	Rgs2	0.022
Gabra5	0.017	Nfkb1	0.007	**Rheb**	**0.091**
Gnai1	**0.075**	Nfkbib	0.001	Sirt1	0.010
Gria1	0.033	Ngf	0.000	Srf	0.006
Gria2	**0.201**	Ngfr	0.002	Synpo	0.008
Gria3	0.036	Nos1	0.004	Timp1	0.004
Gria4	0.057	Nptx2	0.005	Tnf	0.000
Grin1	0.026	Nr4a1	0.005	**Ywhaq**	**0.126**

Table 2: Synaptic plasticity genes organized by category; some genes in multiple categories

Long Term Depression	Long Term Potentiation	Immediate Early Gene	Late Response Gene	Cell Adhesion	Extracellular Matrix & Proteolytic	Creb Cofactor	Neuronal Receptors	Postsynaptic Density	Other
Camk2g	Adcy1	Arc	Inhba,	Adam10	Adam10,	Akt1	Ephb2	Adam10	RGD1562511
Gnai1	Adcy8	Bdnf	Synpo	Cdh2	Mmp9	Camk2g	Gabra5,	Arc	Sirt1
Gria1	Bdnf	Cebpb		Grin2a	Plat	Grin1	Gria1	Dlg4	
Gria2	Camk2a	Cebpd		Grin2b	Reln	Grin2a	Gria2	Gria1	
Gria3	Camk2g	Creb1		Ncam1	Timp1	Grin2b	Gria3	Gria3	
Gria4	Cdh2	Crem		Pcdh8		Grin2c	Gria4	Gria4	
Gria4	Cnr1	Egr1		Ppp2ca		Grin2d	Grin1	Grin1	
Grip1	Gabra5	Egr2		Reln		Mapk1	Grin2a	Grin2a	
Grm1	Gnai1	Egr3		Tnf		Ppp1ca	Grin2b	Grin2b	
Grm2	Gria1	Egr4				Ppp1cc	Grin2c	Grin2c	
Homer1	Gria2	Fos					Grin2d	Grm1	
Igf1	Grin1	Homer1					Grm1	Grm3	
Klf10	Grin2a	Jun					Grm2	Homer1	
Mapk1	Grin2b	Junb					Grm3	Pick1	
Ncam1	Grin2c	Klf10					Grm4	Synpo	
Ngfr	Grin2d	Mmp9					Grm5		
Nos1	Mapk1	Nfkb1					Grm7		
Ntrk2	Mmp9	Nfkbib					Grm8		
Pick1	Ntf4	Ngf					Ntrk2		
Plat	Ntrk2	Nptx2							
Ppp1ca	Plcg1	Nr4a1							
Ppp1cc	Ppp1ca	Ntf3							
Ppp1r14a	Ppp1cc	Pcdh8							
Ppp2ca	Ppp3ca	Pim1							
Ppp3ca	Prkca	Plat							
Prkca	Prkcg	Rela							
Prkg1	Rab3a	Rgs2							
	Ywhaq	Rheb							
		Srf			41				

Table 3: Ipsilateral IC 2-d Post Exposure Fold Change and p Value re Sham Control

Gene	FC	p Value	Gene	FC	p Value	Gene	FC	p Value
Adam10	0.789	0.011	Grin2a	0.917	0.307	Ntf3	0.515	0.008
Adcy1	1.423	0.060	Grin2b	1.016	0.848	Ntf4	0.981	0.919
Adcy8	1.059	0.237	Grin2c	1.365	0.125	Ntrk2	0.917	0.306
Akt1	0.821	0.234	Grin2d	0.804	0.396	Pcdh8	0.943	0.873

Table 6: Contralateral IC 28-d Post Exposure Fold Change and p Value re Sham Control

Gene	FC	p Value	Gene	FC	p Value	Gene	FC	p Value
Adam10	0.550	0.048						
Adcy8	0.679	0.005						
Arc	0.265	0.000						
Bdnf	0.561	0.007						
Camk2a	0.763	0.011						
Camk2g	0.739	0.006						
Cdh2	0.737	0.059						
Cebpb	0.697	0.036						
Cebpd	0.435	0.047						
Cnr1	0.686	0.009						
Creb1	0.731	0.012						
Crem	0.920	0.084						
Dlg4	0.686	0.009						
Egr1	0.415	0.007	Jun	0.736	0.066	Prkg1	0.881	0.106
Egr2	0.353	0.014	Junb	0.265	0.000	Rab3a	0.927	0.000
Egr3	0.435	0.006	Klf10	0.552	0.001	Rela	0.778	0.079
Egr4	0.506	0.002	Mapk1	0.973	0.398	Reln	0.691	0.015
Ephb2	0.602	0.004	Mmp9	0.642	0.002	RGD1562511	0.652	0.012
Fos	0.279	0.000	Ncam1	0.719	0.006	Rgs2	0.822	0.000
Gabra5	0.746	0.009	Nfkb1	0.571	0.003	Rheb	0.923	0.002
Gnai1	0.867	0.107	Nfkbib	0.662	0.184	Sirt1	0.843	0.004
Gria1	0.652	0.013	Ngf	0.612	0.009	Srf	0.699	0.012
Gria2	0.841	0.101	Ngfr	0.417	0.000	Synpo	0.826	0.111
Gria3	0.873	0.054	Nos1	0.688	0.006	Timp1	0.620	0.000
Gria4	0.914	0.005	Nptx2	0.561	0.001	Tnf	0.422	0.024
Grin1	0.593	0.002	Nr4a1	0.371	0.000	Ywhaq	0.897	0.027

28-d post-exposure